PERGAMON

International Journal of Solids and Structures 40 (2003) 2487–2499

INTERNATIONAL JOURNAL OF SOLIDS and STRUCTURES

www.elsevier.com/locate/ijsolstr

A structural mechanics approach for the analysis of carbon nanotubes

Chunyu Li, Tsu-Wei Chou *

Department of Mechanical Engineering, Center for Composite Materials, University of Delaware, 126 Spencer Laboratory, Newark, DE 19716-3140, USA

Received 14 March 2002; received in revised form 3 January 2003

Abstract

This paper presents a structural mechanics approach to modeling the deformation of carbon nanotubes. Fundamental to the proposed concept is the notion that a carbon nanotube is a geometrical frame-like structure and the primary bonds between two nearest-neighboring atoms act like load-bearing beam members, whereas an individual atom acts as the joint of the related load-bearing beam members. By establishing a linkage between structural mechanics and molecular mechanics, the sectional property parameters of these beam members are obtained. The accuracy and stability of the present method is verified by its application to graphite. Computations of the elastic deformation of single-walled carbon nanotubes reveal that the Young's moduli of carbon nanotubes vary with the tube diameter and are affected by their helicity. With increasing tube diameter, the Young's moduli of both armchair and zigzag carbon nanotubes increase monotonically and approach the Young's modulus of graphite. These findings are in good agreement with the existing theoretical and experimental results.

Keywords: Carbon nanotube; Nanomechanics; Molecular mechanics; Force fields; Atomistic modeling; Structural mechanics

1. Introduction

The advancement of science and technology has evolved into the era of nanotechnology. The most distinct characteristic of nanotechnology is that the properties of nanomaterials are size-dependent. Due to the extremely small size of nanomaterials, the evaluation of their mechanical properties, such as elastic modulus, tensile/compressive strength and buckling resistance, presents significant challenges to researchers in nanomechanics. While the experimental works has brought about striking progress in the research of nanomaterials, many researchers have also resorted to the computational nanomechanics. Because computer simulations based on reasonable physical models cannot only highlight the molecular features of nanomaterials for theoreticians but also provide guidance and interpretations for experimentalists. It is still

* Corresponding author. Tel.: +1-302-831-2423/2421; fax: +1-302-831-3619.
E-mail address: chou@me.udel.edu (T.-W. Chou).

0020-7683/03/$ - see front matter © 2003 Elsevier Science Ltd. All rights reserved.
doi:10.1016/S0020-7683(03)00056-8

an ongoing and challenging process to identify effective and efficient computational methods with respect to specific nanomaterials.

Among the many nanostructured materials, carbon nanotubes have attracted considerable attention. This kind of long and slender fullerene was first discovered by Iijima (1991). They can be produced by an array of techniques, such as arc discharge, laser ablation and chemical vapor deposition. A recent review of the processing and properties of carbon nanotubes and their composites is given by Thostenson et al. (2001). From the viewpoint of atomic arrangement, carbon nanotubes can be visualized as cylinders that rolled from sheets of graphite. They assume either single-walled or multi-walled structures and their helicity may also be different (Iijima and Ichlhashi, 1993; Bethune et al., 1993). Since the discovery of carbon nanotubes, much attention has been given to the investigation of their exceptional physical properties (Thostenson et al., 2001; Harris, 1999). It has been revealed that the conducting properties of carbon nanotubes depend dramatically on their helicity and diameter (Terrones et al., 1999), and the stiffness, flexibility and strength of carbon nanotubes are much higher than those of conventional carbon fibers (Treacy et al., 1996; Salvetat et al., 1999; Iijima et al., 1996). The extraordinary properties of carbon nanotubes have motivated researchers worldwide to study the fundamentals of this novel material as well as to explore their applications in different fields (Ajayan and Zhou, 2001).

Besides the great deal of experimental works on carbon nanotubes, many researchers have pursued the analysis of carbon nanotubes by theoretical modeling (Harris, 1999; Saito et al., 1998). These modeling approaches can be generally classified into two categories. One is the atomistic modeling and the major techniques include classical molecular dynamics (MD) (Iijima et al., 1996; Yakobson et al., 1997), tight-binding molecular dynamics (TBMD) (Hernandez et al., 1998) and density functional theory (DFT) (Sanchez-Portal et al., 1999). In principle, any problem associated with molecular or atomic motions can be simulated by these modeling techniques. However, due to their huge computational tasks, practical applications of these atomistic modeling techniques are limited to systems containing a small number of molecules or atoms and are usually confined to studies of relatively short-lived phenomena, from picoseconds to nanoseconds.

The other approach is the continuum mechanics modeling. Some researchers have resorted to classical continuum mechanics for modeling carbon nanotubes. For examples, Tersoff (1992) conducted simple calculations of the energies of fullerenes based on the deformation of a planar graphite sheet, treated as an elastic continuum, and concluded that the elastic properties of the graphite sheet can be used to predict the elastic strain energy of fullerenes and nanotubes. Yakobson et al. (1996) noticed the unique features of fullerenes and developed a continuum shell model. Ru (2000a,b) followed this continuum shell model to investigate buckling of carbon nanotubes subjected to axial compression. This kind of continuum shell models can be used to analyze the static or dynamic mechanical properties of nanotubes. However, these models neglect the detailed characteristics of nanotube chirality, and are unable to account for forces acting on the individual atoms.

Therefore, there is a demand of developing a modeling technique that analyzes the mechanical response of nanotubes at the atomistic scale but is not perplexed in time scales. Such a modeling approach would benefit us in novel nanodevices design and multi-scale simulations of nanosystems (Nakano et al., 2001). In this paper, we extend the theory of classical structural mechanics into the modeling of carbon nanotubes. Our idea stems from that carbon nanotubes are elongated fullerenes, which were named after the architect known for designing geodesic domes, R. Buckmister Fuller. In fact, it is obvious that there are some similarities between the molecular model of a nanotube and the structure of a frame building. In a carbon nanotube, carbon atoms are bonded together by covalent bonds. These bonds have their characteristic bond lengths and bond angles in a three-dimensional space. Thus, it is logical to simulate the deformation of a nanotube based on the method of classical structural mechanics. In following sections, we first establish the bases of this concept and then demonstrate the approach by a few computational examples.

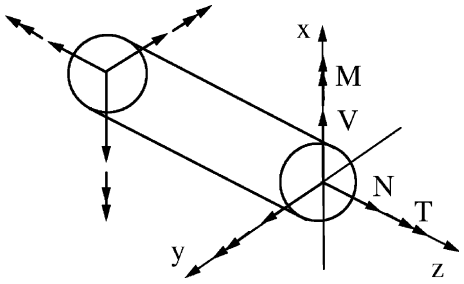

Fig. 1. Illustration of a beam element in a space frame.

2. Brief review of structural mechanics for space frames

Structural mechanics analysis enables the determination of the displacements, strains and stresses of a structure under given loading conditions. Of the various modern structural analysis techniques, the stiffness matrix method has been by far the most generally used. The method can be readily applied to analyze structures of any geometry and can be used to solve linear elastic static problems as well as problems involving buckling, plasticity and dynamics. In the following, we briefly review the stiffness matrix method for linearly elastic space frame problems, which is relevant to the present studies.

For an element in a space frame as shown in Fig. 1, the elemental equilibrium equation can be written as following (Weaver and Gere, 1990):

$$\mathbf{K}\mathbf{u} = \mathbf{f}, \tag{1}$$

where

$$\mathbf{u} = [u_{xi}, u_{yi}, u_{zi}, \theta_{xi}, \theta_{yi}, \theta_{zi}, u_{xj}, u_{yj}, u_{zj}, \theta_{xj}, \theta_{yj}, \theta_{zj}]^{\mathrm{T}}, \tag{2}$$

$$\mathbf{f} = [f_{xi}, f_{yi}, f_{zi}, m_{xi}, m_{yi}, m_{zi}, f_{xj}, f_{yj}, f_{zj}, m_{xj}, m_{yj}, m_{zj}]^{\mathrm{T}} \tag{3}$$

are the nodal displacement vector and nodal force vector of the element, respectively and $\mathbf{K}$ is the elemental stiffness matrix. The matrix $\mathbf{K}$ consists of following submatrices:

$$\mathbf{K} = \begin{bmatrix} \mathbf{K}_{ii} & \mathbf{K}_{ij} \\ \mathbf{K}_{ij}^{\mathrm{T}} & \mathbf{K}_{jj} \end{bmatrix}, \tag{4}$$

where

$$\mathbf{K}_{ii} = \begin{bmatrix} EA/L & 0 & 0 & 0 & 0 & 0 \\ 0 & 12EI_x/L^3 & 0 & 0 & 0 & 6EI_x/L^2 \\ 0 & 0 & 12EI_y/L^3 & 0 & -6EI_y/L^2 & 0 \\ 0 & 0 & 0 & GJ/L & 0 & 0 \\ 0 & 0 & -6EI_y/L^2 & 0 & 4EI_y/L & 0 \\ 0 & 6EI_x/L^2 & 0 & 0 & 0 & 4EI_x/L \end{bmatrix}, \tag{5}$$

$$\mathbf{K}_{ij} = \begin{bmatrix} -EA/L & 0 & 0 & 0 & 0 & 0 \\ 0 & -12EI_x/L^3 & 0 & 0 & 0 & 6EI_x/L^2 \\ 0 & 0 & -12EI_y/L^3 & 0 & -6EI_y/L^2 & 0 \\ 0 & 0 & 0 & -GJ/L & 0 & 0 \\ 0 & 0 & 6EI_y/L^2 & 0 & 2EI_y/L & 0 \\ 0 & -6EI_x/L^2 & 0 & 0 & 0 & 2EI_x/L \end{bmatrix}, \tag{6}$$

$$\mathbf{K}_{jj} = \begin{bmatrix} EA/L & 0 & 0 & 0 & 0 & 0 \\ 0 & 12EI_x/L^3 & 0 & 0 & 0 & -6EI_x/L^2 \\ 0 & 0 & 12EI_y/L^3 & 0 & 6EI_y/L^2 & 0 \\ 0 & 0 & 0 & GJ/L & 0 & 0 \\ 0 & 0 & 6EI_y/L^2 & 0 & 4EI_y/L & 0 \\ 0 & -6EI_x/L^2 & 0 & 0 & 0 & 4EI_x/L \end{bmatrix}. \tag{7}$$

It is observed from the above elemental stiffness matrices that when the length, L, of the element is known, there are still four stiffness parameters need to be determined. They are the tensile resistance EA, the flexural rigidity EI_x and EI_y and the torsional stiffness GJ. In order to obtain the deformation of a space frame, the above elemental stiffness equations should be established for every element in the space frame and then all these equations should be transformed from the local coordinates to a common global reference system. Finally, a system of simultaneous linear equations can be assembled according to the requirements of nodal equilibrium. By solving the system of equations and taking into account the boundary restraint conditions, the nodal displacements can be obtained.

3. Structural characteristics of carbon nanotubes

A single-walled carbon nanotube (SWNT) can be viewed as a graphene sheet that has been rolled into a tube. A multi-walled carbon nanotube (MWNT) is composed of concentric graphitic cylinders with closed caps at both ends and the graphitic layer spacing is about 0.34 nm. Unlike diamond, which assumes a 3-D crystal structure with each carbon atom having four nearest neighbors arranged in a tetrahedron, graphite assumes the form of a 2-D sheet of carbon atoms arranged in a hexagonal array. In this case, each carbon atom has three nearest neighbors.

The atomic structure of nanotubes can be described in terms of the tube chirality, or helicity, which is defined by the chiral vector $\vec{C}_h$ and the chiral angle θ. In Fig. 2, we can visualize cutting the graphite sheet along the dotted lines and rolling the tube so that the tip of the chiral vector touches its tail. The chiral vector, also known as the roll-up vector, can be described by the following equation:

$$\vec{C}_h = n\vec{a}_1 + m\vec{a}_2, \tag{8}$$

where the integers (n, m) are the number of steps along the zigzag carbon bonds of the hexagonal lattice and $\vec{a}_1$ and $\vec{a}_2$ are unit vectors. The chiral angle determines the amount of 'twist' in the tube. The chiral angles are 0° and 30° for the two limiting cases which are referred to as zigzag and armchair, respectively (Fig. 3).

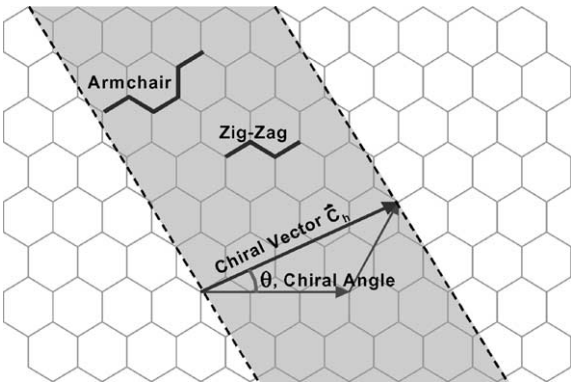

Fig. 2. Schematic diagram of a hexagonal graphene sheet (Thostenson et al., 2001).

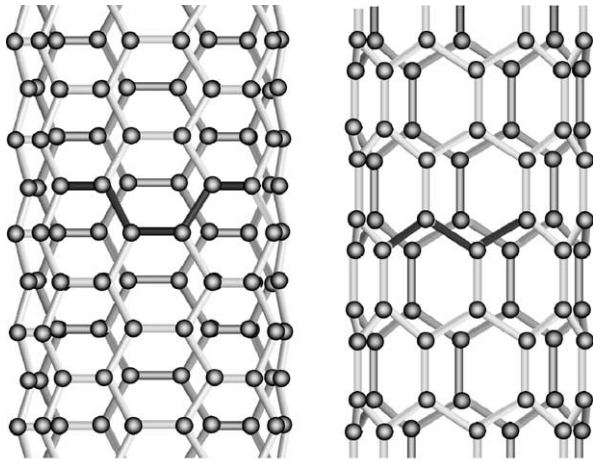

Fig. 3. Schematic diagram of (a) an armchair and (b) a zigzag nanotube (Thostenson et al., 2001).

In terms of the roll-up vector, the zigzag nanotube is denoted by $(n, 0)$ and the armchair nanotube (n, n). The roll-up vector of the nanotube also defines the nanotube diameter.

The physical properties of carbon nanotubes are sensitive to their diameter, length and chirality. In particular, tube chirality is known to have a strong influence on the electronic properties of carbon nanotubes. Graphite is considered to be a semi-metal, but it has been shown that nanotubes can be either metallic or semi-conducting, depending on tube chirality (Dresselhaus et al., 1996). The influence of chirality on the mechanical properties of carbon nanotubes has also been reported (Popov et al., 2000; Hernandez et al., 1998).

4. Structural mechanics approach to carbon nanotubes

From the structural characteristics of carbon nanotubes, it is logical to anticipate that there are potential relations between the deformations of carbon nanotubes and frame-like structures. For macroscopic space frame structures made of practical engineering materials, the material properties and element sectional parameters can be easily obtained from material data handbooks and calculations based on the element sectional dimensions. For nanoscopic carbon nanotubes, there is no information about the elastic and sectional properties of the carbon–carbon bonds and the material properties. Therefore, It is imperative to establish a linkage between the microscopic computational chemistry and the macroscopic structural mechanics.

4.1. Potential functions of molecular mechanics

From the viewpoint of molecular mechanics, a carbon nanotube can be regarded as a large molecule consisting of carbon atoms. The atomic nuclei can be regarded as material points. Their motions are regulated by a force field, which is generated by electron–nucleus interactions and nucleus–nucleus interactions (Machida, 1999). Usually, the force field is expressed in the form of steric potential energy. It depends solely on the relative positions of the nuclei constituting the molecule. The general expression of

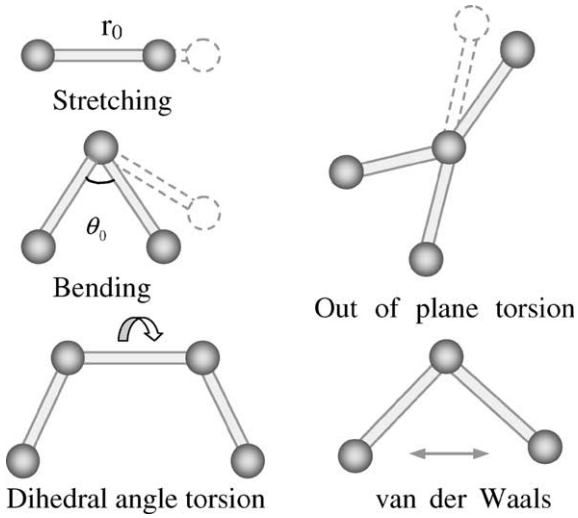

Fig. 4. Interatomic interactions in molecular mechanics.

the total steric potential energy, omitting the electrostatic interaction, is a sum of energies due to valence or bonded interactions and nonbonded interactions (Rappe et al., 1992):

$$U = \sum U_r + \sum U_\theta + \sum U_\phi + \sum U_\omega + \sum U_{\text{vdw}}, \tag{9}$$

where U_r is for a bond stretch interaction, U_θ for a bond angle bending, U_ϕ for a dihedral angle torsion, U_ω for an improper (out-of-plane) torsion, U_{vdw} for a nonbonded van der Waals interaction, as shown in Fig. 4.

There has been a wealth of literature in molecular mechanics devoted to finding the reasonable functional forms of these potential energy terms (Rappe et al., 1992; Brenner, 1990; Mayo et al., 1990; Cornell et al., 1995). Therefore, various functional forms may be used for these energy terms, depending on the particular material and loading conditions considered. In general, for covalent systems, the main contributions to the total steric energy come from the first four terms, which have included four-body potentials. Under the assumption of small deformation, the harmonic approximation is adequate for describing the energy (Gelin, 1994). For sake of simplicity and convenience, we adopt the simplest harmonic forms and merge the dihedral angle torsion and the improper torsion into a single equivalent term, i.e.,

$$U_r = \tfrac{1}{2}k_r(r - r_0)^2 = \tfrac{1}{2}k_r(\Delta r)^2, \tag{10}$$

$$U_\theta = \tfrac{1}{2}k_\theta(\theta - \theta_0)^2 = \tfrac{1}{2}k_\theta(\Delta\theta)^2, \tag{11}$$

$$U_\tau = U_\phi + U_\omega = \tfrac{1}{2}k_\tau(\Delta\phi)^2, \tag{12}$$

where k_r, k_θ and k_τ are the bond stretching force constant, bond angle bending force constant and torsional resistance respectively, and the symbols Δr, $\Delta\theta$ and $\Delta\phi$ represent the bond stretching increment, the bond angle change and the angle change of bond twisting, respectively.

4.2. Linkage between sectional stiffness parameters and constants of force fields

In a carbon nanotube, the carbon atoms are bonded to each other by covalent bonds and form hexagons on the wall of the tube. These covalent bonds have their characteristic bond lengths and bond angles in a

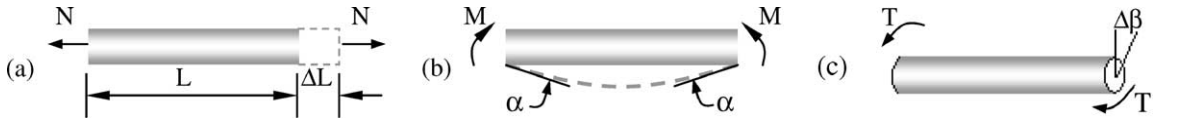

Fig. 5. Pure tension, bending and torsion of an element.

three-dimensional space. When a nanotube is subjected to external forces, the displacements of individual atoms are constrained by these bonds. The total deformation of the nanotube is the result of these bond interactions. By considering the covalent bonds as connecting elements between carbon atoms, a nanotube could be simulated as a space frame-like structure. The carbon atoms act as joints of the connecting elements.

In the following, we establish the relations between the sectional stiffness parameters in structural mechanics and the force constants in molecular mechanics. For convenience, we assume that the sections of carbon–carbon bonds are identical and uniformly round. Thus it can be assumed that $I_x = I_y = I$ and only three stiffness parameters, EA, EI and GJ, need to be determined.

Because the deformation of a space frame results in the changes of strain energies, we determine the three stiffness parameters based on the energy equivalence. Notice that each of the energy terms in molecular mechanics (Eqs. (10)–(12)) represents an individual interaction and no cross-interactions are included, we also need to consider the strain energies of structural elements under individual forces. According to the theory of classical structural mechanics, the strain energy of a uniform beam of length L subjected to pure axial force N (Fig. 5a) is

$$U_A = \frac{1}{2}\int_0^L \frac{N^2}{EA}\,\mathrm{d}L = \frac{1}{2}\frac{N^2 L}{EA} = \frac{1}{2}\frac{EA}{L}(\Delta L)^2, \tag{13}$$

where ΔL is the axial stretching deformation. The strain energy of a uniform beam under pure bending moment M (Fig. 5b) is

$$U_M = \frac{1}{2}\int_0^L \frac{M^2}{EI}\,\mathrm{d}L = \frac{2EI}{L}\alpha^2 = \frac{1}{2}\frac{EI}{L}(2\alpha)^2, \tag{14}$$

where α denotes the rotational angle at the ends of the beam. The strain energy of a uniform beam under pure torsion T (Fig. 5c) is

$$U_T = \frac{1}{2}\int_0^L \frac{T^2}{GJ}\,\mathrm{d}L = \frac{1}{2}\frac{T^2 L}{GJ} = \frac{1}{2}\frac{GJ}{L}(\Delta\beta)^2, \tag{15}$$

where $\Delta\beta$ is the relative rotation between the ends of the beam.

It can be seen that in Eqs. (10)–(15) both U_r and U_A represent the stretching energy, both U_θ and U_M represent the bending energy, and both U_τ and U_T represent the torsional energy. It is reasonable to assume that the rotation angle 2α is equivalent to the total change $\Delta\theta$ of the bond angle, ΔL is equivalent to Δr, and $\Delta\beta$ is equivalent to $\Delta\phi$. Thus by comparing Eqs. (10)–(12) and Eqs. (13)–(15), a direct relationship between the structural mechanics parameters EA, EI and GJ and the molecular mechanics parameters k_r, k_θ and k_τ is deduced as following:

$$\frac{EA}{L} = k_r, \quad \frac{EI}{L} = k_\theta, \quad \frac{GJ}{L} = k_\tau. \tag{16}$$

Eq. (16) establishes the foundation of applying the theory of structural mechanics to the modeling of carbon nanotubes or other similar fullerene structures. As long as the force constants k_r, k_θ and k_τ are known, the sectional stiffness parameters EA, EI and GJ can be readily obtained. And then by following the

solution procedure of stiffness matrix method for frame structures, the deformation and related elastic behavior of graphene sheets and nanotubes at the atomistic scale can be simulated.

5. Results and discussions

To verify the reliability and efficiency of the structural mechanics approach to the modeling of carbon nanotubes and to demonstrate its capability, we choose graphite sheets and single-walled carbon nanotubes as examples and calculate some of their basic elastic properties, such as Young's modulus and shear modulus. In these computations, the initial carbon–carbon bond length is taken as 1.421 Å (Dresselhaus et al., 1995). The computational results are compared with the limited existing theoretical and experimental results.

5.1. Young's modulus of a graphene sheet

As stated earlier, a carbon nanotube can be viewed as a sheet of graphite that has been rolled into a tube. Thus, we first calculate the Young's modulus of a graphene sheet (Fig. 6a) to verify the feasibility of the present method. It is also expected that these calculations can provide useful information concerning the selection of force field constants.

The Young's modulus of a material is the ratio of the normal stress to the normal strain in a uniaxial tension test

$$Y = \frac{\sigma}{\varepsilon} = \frac{F/A_0}{\Delta H/H_0}, \tag{17}$$

where F stands for the total force acting on the atoms at one end of the sheet, $A_0 = Wt$ is the cross-sectional area of the sheet with width W and thickness t, H_0 is the initial length and ΔH its elongation. The thickness t is taken as the interlayer spacing of graphite, 0.34 nm (Dresselhaus et al., 1995).

Table 1 lists the computed Young's modulus of a graphene sheet for different model sizes and different force field parameters, which are selected from AMBER (Cornell et al., 1995). It can be seen that our results from both pairs of force field constants are fairly close to the commonly accepted value (1.025 TPa) (Kelly, 1981) of the Young's modulus of graphite. Furthormore, our results are very close to the recent prediction (1.029 TPa) based on ab initio computation (Kudin et al., 2001). It is also observed in Table 1 that the computational results are weakly affected by model size.

5.2. Young's modulus of a single-walled carbon nanotube

The successful prediction of the Young's moduli of graphene sheets established our confidence in applying this method to analyzing the Young's modulus of carbon nanotubes. Two main types of carbon nanotubes, i.e., armchair and zigzag, are considered. The force constant values are chosen based upon the experience with graphite sheets: $k_r/2 = 469$ kcal mol^{-1} Å^{-2}, $k_\theta/2 = 63$ kcal mol^{-1} rad^{-2}. The force constant k_τ is adopted as $k_\tau/2 = 20$ kcal mol^{-1} rad^{-2} based on references (Cornell et al., 1995; Jorgensen and Severance, 1990). There is no test data for optimizing the choice of k_τ. But our calculation showed that the influence of k_τ on carbon nanotube Young's modulus is very weak. The tensile force is applied on one end of a carbon nanotube and the other end is fixed (Fig. 6b). Eq. (17) is still used for calculating the Young's modulus, except that the sectional area is now $A_0 = \pi dt$ with d standing for the tube diameter.

Fig. 7 displays the variations of the Young's modulus with nanotube diameter. It can be seen that the trend is similar for both armchair and zigzag SWNTs, and the effect of nanotube chirality is not significant. For tube diameters larger than 0.7 nm, the Young's moduli of zigzag nanotubes become slightly larger than

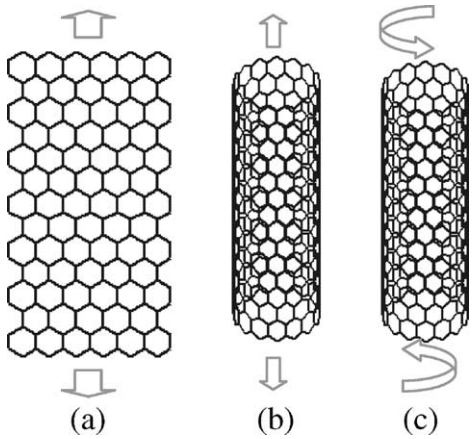

Fig. 6. Computational models of a graphene sheet and single-walled carbon nanotubes.

Table 1
The variation of Young's modulus of a graphene sheet with force field constants k_r (kcal mol^{-1} Å^{-2}) and k_θ (kcal mol^{-1} rad^{-2}), and model size

Model size (nm)		$\frac{1}{2}k_r$, $\frac{1}{2}k_\theta$	
Width	Height	469, 63	447, 70
		Young's modulus (TPa)	
0.738	2.842	0.995	1.002
0.985	3.126	1.002	1.008
1.969	4.831	1.021	1.022
1.969	9.847	1.024	1.023
4.184	20.178	1.033	1.030

those of armchair nanotubes, and the trend is reversed for tube diameters less than 0.7 nm. This correlation between nanotube chirality and Young's modulus can be understood from interatomic bond orientation. In zigzag nanotubes, one-third of the bonds are aligned with the loading direction, while every bond is at an angle with the loading axis in armchair nanotubes. Thus the difference in nanotube elastic behavior is a direct consequence of the intrinsic atomic structure. When the tube diameter is very smaller, the distortion of C–C bonds of zigzag nanotubes may be more significant than that of armchair nanotubes. Therefore, the Young's modulus of the former is slightly less than that of the latter.

From Fig. 7, the effect of tube diameter on the Young's modulus is also clearly observed. For smaller tube, for example, diameter less than 1.0 nm, the Young's modulus exhibits a strong dependence on the tube diameter. The maximum relative difference reaches 6–12%. However, for tube diameters larger than 1.0 nm, this dependence becomes very weak. The maximum relative difference is less than 3%. The general tendency is that the Young's modulus increases with increasing tube diameter. The lower Young's modulus at smaller nanotube diameter is attributed to the higher curvature, which results in a more significant distortion of C–C bonds. As the nanotube diameter increases, the effect of curvature diminishes gradually, and the Young's modulus approaches to that of graphite as predicted by the present method as well as that reported in the literature (Kelly, 1981).

Our computational results are comparable to those obtained from experiments. Wong et al. (1997) obtained the Young's moduli of carbon MWNTs of 1.28 ± 0.59 TPa by using atomic force microscopy based experiments. Salvetat et al. (1999) reported the Young's modulus values of carbon MWNTs to be

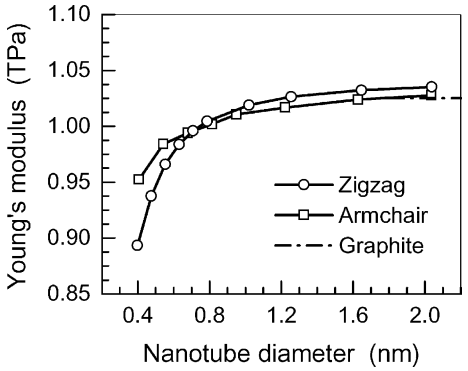

Fig. 7. Young's moduli of carbon nanotubes versus tube diameter.

0.81 ± 0.41 TPa by the same experimental technique. Krishnan et al. (1998) measured single-walled carbon nanotubes (SWNTs) and obtained an average Young's modulus of 1.25 TPa. Our predictions are in reasonable agreement with these experimental results.

Furthermore, our computational results are also comparable to the theoretical results provided by other modeling techniques. Lu (1997) and Popov et al. (2000) obtained the Young's moduli of SWNTs of about 1 TPa by using the empirical lattice dynamics model. By a nonorthogonal tight-binding molecular dynamics simulation, Hernandez et al. (1998) revealed the dependency of the Young's modulus on nanotube diameter and chirality and gave an average value of 1.24 TPa. Finally, for a range of SWNTs, ab initio calculation with a pseudo-potential density functional theory (DFT) showed that average value of the second derivative of strain energy with respect to the axial strain is 56 eV, which is nearly identical to that of graphite (56.3 eV) (Sanchez-Portal et al., 1999). Compared with ab initio studies (Sanchez-Portal et al., 1999; Van Lier et al., 2000; Kudin et al., 2001), the empirical lattice dynamics analysis (Lu, 1997; Popov et al., 2000) and the tight-binding molecular dynamics simulations (Hernandez et al., 1998), the present results are also in reasonable agreement with those reviewed above.

5.3. Shear modulus of a single-walled carbon nanotube

Due to the difficulty in experimental techniques, there is still no report on the measured values of shear modulus of carbon nanotubes. Theoretical predictions on the shear modulus of carbon nanotubes are also very few. Lu (1997) predicted the shear modulus for carbon SWNTs by using empirical lattice dynamics model, and concluded that the shear modulus ($\sim$0.5 TPa) is comparable to that of diamond and is insensitive to tube diameter and tube chirality. Popov et al. (2000) also used the lattice-dynamics model and derived an analytical expression for the shear modulus. Their results indicated that the shear moduli of carbon SWNTs are about equal to that of graphite for large radii but are less than that of graphite at small radii, and the tube chirality has some effect on the shear modulus for small tube radii.

In the present work, a carbon SWNT is assumed to be subjected to a torsional moment at one end and is constrained at the other end (Fig. 6c). The following formula, which is based on the theory of elasticity at the macroscopic scale, is used for obtaining the shear modulus:

$$S = \frac{TL_0}{\theta J_0}, \tag{18}$$

where T stands for the torque acting at the end of an SWNT, L_0 is the length of the tube, θ is the torsional angle and J_0 for the cross-sectional polar inertia of the SWNT. In the calculation of the polar inertia J_0, the SWNT is treated as a hollow tube with a wall thickness of 0.34 nm.

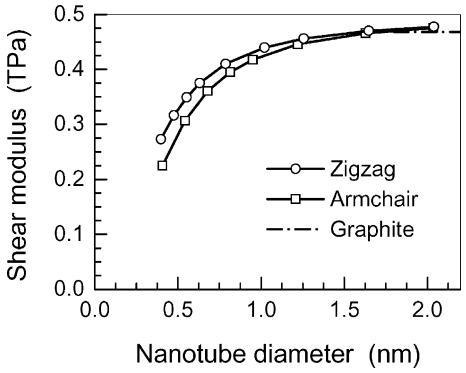

Fig. 8. Shear moduli of carbon nanotubes versus tube diameter.

Fig. 8 illustrates the computational results for armchair and zigzag SWNTs. It is observed that the shear modulus behaves similarly to the Young's modulus in that it increases with increasing tube diameter for small tube diameters. At larger diameters (e.g., >2 nm), the shear modulus becomes insensitive to tube diameter. For the range of tube diameter considered, the effect of tube chirality on the shear modulus is not significant. For tube diameters larger than 2.0 nm, the shear moduli of armchair and zigzag SWNTs are almost the same. By comparing our findings with existing results (Lu, 1997; Popov et al., 2000), it can be concluded that the present method can achieve the same accuracy as other existing methods.

5.4. Discussions

We have introduced the structural mechanics approach to modeling carbon nanotubes. Our purpose of proposing such an approximate method is to explore nanoscale problems with existing theories of solid mechanics and methods of computational mechanics. Building on the fundamental concept developed here, we expect to also address the strength and buckling of single-walled carbon nanotubes. We also plan to further develop the concept of this approach into the modeling of multi-walled carbon nanotubes. However, the versatility of the present approach relies very much on the development of modern computational chemistry. The feasibility of applying the present approach to modeling other nanotubes, such as boron nitride, or other covalent materials, such as silicon and diamond, would depend on the availability and accuracy of force field parameters of these materials.

Compared with other refined atomistic simulation methods, such as classical molecular dynamics or tight-binding molecular dynamics, the present approach possesses two advantages. First, it can be used for simulating both static and dynamic loadings. Second, since it does not consider thermal vibration of the atoms and treats only "long time" phenomena, the economy in computation is achieved through such simplifications.

In the establishment of relationship between structural mechanics parameters and force field constants, some approximations are made. We recognize the uncertainty in rigorously defining the angles of bond bending and torsion when a chemical bond is treated as a beam because the theory of structural mechanics and the theory of molecular mechanics have very different bases. However, by approximating the equivalence in energy terms stem from similar deformations in structural mechanics and molecular mechanics, we circumvented the need in determining the bond angle changes due to bending and torsion. For the equivalence of bending energy terms, we split the change of bond angle in molecular mechanics into the beam rotations at two beam-ends in structural mechanics. The combination of energy terms due to out-of-plane torsion and dihedral angle torsion is done simply from the viewpoint that both involve torsional

deformation. But the main contribution is from dihedral torsion, and also for the purpose of obtaining the torsional rigidity of the beam element, we assume that U_τ has the functional form of dihedral torsion. Through the approximation of equaling U_τ and U_T, the effect of out-of-plane torsion is reflected in the parameter of k_τ. Our computational experience indicates that the out-of-plane torsion is insignificant and the error introduced due to this approximation is negligible.

Another issue that should be addressed is the wall thickness of single-walled carbon nanotube. We have noticed there were different assumptions of the thickness, such as 0.34 nm (Lu, 1997), 0.066 nm (Yakobson et al., 1997) and 0.0894 nm (Kudin et al., 2001). A detailed discussion of this issue has been given by Yakobson and Avouris (2001). Considering the relationship between graphite and multi-walled carbon nanotubes and for the purpose of comparing their elastic properties, we assumed the thickness of a single-walled carbon nanotube to be the same as the interlayer spacing of graphite (0.34 nm).

6. Conclusions

A structural mechanics approach has been developed for modeling carbon nanotubes. A simple linkage between structural mechanics and molecular mechanics is established. In this approach, the computational strategy is essentially classical structural mechanics, but the theoretical concept stems from modern computational chemistry and the modeling is kept at the atomistic scale. Our computational results for elastic properties of carbon nanotubes are comparable to those obtained from other modeling techniques. The major advantages of our method are the simplicity of the concept and the improved computational efficiency for analyzing the deformation of carbon nanotubes. It is expected that the present methodology will be further developed to model other covalent-bonded materials and facilitate analysis of the deformation of nanotube-based composites.

Acknowledgements

This paper is dedicated to Professor William D. Nix. This work is partially supported by the National Science Foundation (ECS-0103012, Dr. Usha Varshney, Program Director) and the Army Research Office (DAAD 19-02-1-0264, Dr. Bruce LaMattina, Program Director).

References

Ajayan, P.M., Zhou, O.Z., 2001. Application of carbon nanotubes. Topics in Applied Physics 80, 391–425.

Bethune, D.S., Kiang, C.H., Devries, M.S., Gorman, G., Savoy, R., Vazquez, J., et al., 1993. Cobaltcatalyzed growth of carbon nanotubes with single-atomic-layer walls. Nature 363, 605–607.

Brenner, D.W., 1990. Empirical potential for hydrocarbons for use in simulating the chemical vapor deposition of diamond films. Physical Review B 42, 9458.

Cornell, W.D., Cieplak, P., Bayly, C.I., et al., 1995. A second generation force-field for the simulation of proteins, nucleic-acids, and organic-molecules. Journal of American Chemical Society 117, 5179–5197.

Dresselhaus, M.S., Dresselhaus, G., Saito, R., 1995. Physics of carbon nanotubes. Carbon 33, 883.

Dresselhaus, M.S., Dresselhaus, G., Eklund, P.C., 1996. Science of Fullerenes and Carbon Nanotubes. Academic Press, San Diego.

Gelin, B.R., 1994. Molecular Modeling of Polymer Structures and Properties. Hanser/Gardner Publishers, Cincinnati.

Harris, P.J.F., 1999. Carbon Nanotubes and Related Structures. Cambridge University Press, UK.

Hernandez, E., Goze, C., Bernier, P., Rubio, A., 1998. Elastic properties of C and BxCyNz composite nanotubes. Physical Review Letters 80, 4502–4505.

Iijima, S., 1991. Helical microtubules of graphitic carbon. Nature 354, 56–58.

Iijima, S., Ichlhashi, T., 1993. Single-shell carbon nanotubes of 1-nm diameter. Nature 363, 603–605.

Iijima, S., Brabec, C., Maiti, A., Bernholc, J., 1996. Structural flexibility of carbon nanotubes. Journal of Chemical Physics 104, 2089–2092.

Jorgensen, W.L., Severance, D.L., 1990. Aromatic aromatic interactions—free-energy profiles for the benzene dimer in water, chloroform, and liquid benzene. Journal of American Chemical Society 112, 4768–4774.

Kelly, B.T., 1981. Physics of Graphite. Applied Science, London.

Krishnan, A. et al., 1998. Young's modulus of single-walled nanotubes. Physical Review B 58, 14013–14019.

Kudin, K.N., Scuseria, G.E., Yakobson, B.I., 2001. C_2F, BN and C nanoshell elasticity from ab initio computations. Physical Review B 64, 235406.

Lu, J.P., 1997. Elastic properties of carbon nanotubes and nanoropes. Physical Review Letters 79, 1297–1300.

Machida, K., 1999. Principles of Molecular Mechanics. Kodansha and John Wiley & Sons Co-publication, Tokyo.

Mayo, S.L., Olafson, B.D., Goddard, W.A., 1990. Dreiding—a generic force-field for molecular simulations. Journal of Physical Chemistry 94, 8897–8909.

Nakano, A. et al., 2001. Multiscale simulation of nanosystems. Computing in Science and Engineering 3, 56–66.

Popov, V.N., Van Doren, V.E., Balkanski, M., 2000. Elastic properties of single-walled carbon nanotubes. Physical Review B 61, 3078–3084.

Rappe, A.K., Casewit, C.J., Colwell, K.S., et al., 1992. UFF, A full periodic-table force-field for molecular mechanics and molecular dynamics simulations. Journal of American Chemical Society 114, 10024–10035.

Ru, C.Q., 2000a. Effective bending stiffness of carbon nanotubes. Physical Review B 62, 9973–9976.

Ru, C.Q., 2000b. Elastic buckling of single-walled carbon nanotube ropes under high pressure. Physical Review B 62, 10405–10408.

Saito, S., Dresselhaus, D., Dresselhaus, M.S., 1998. Physical Properties of Carbon Nanotubes. Imperical College Press, London.

Salvetat, J.P., Bonard, J.M., Thomson, N.H., Kulik, A.J., Forró, L., Benoit, W., Zuppiroli, L., 1999. Mechanical properties of carbon nanotubes. Applied Physics A 69, 255–260.

Sanchez-Portal, D. et al., 1999. Ab initio structural, elastic, and vibrational properties of carbon nanotubes. Physical Review B 59, 12678–12688.

Terrones, M., Hsu, W.K., Kroto, H.W., Walton, D.R.M., 1999. Nanotubes: a revolution in materials science and electronics. Topic in current Chemistry 199, 190–234.

Tersoff, J., 1992. Energies of fullerenes. Physical Review B 46, 15546–15549.

Thostenson, E.T., Ren, Z., Chou, T.-W., 2001. Advances in the science and technology of carbon nanotubes and their composites: a review. Composites Science and Technology 61, 1899–1912.

Treacy, M.M.J., Ebbesen, T.W., Gibson, T.M., 1996. Exceptionally high Young's modulus observed for individual carbon nanotubes. Nature 381, 680–687.

Van Lier, G. et al., 2000. Ab initio study of the elastic properties of single-walled carbon nanotubes and graphene. Chemical Physical Letters 326, 181–185.

Weaver Jr., W., Gere, J.M., 1990. Matrix Analysis of Framed Structures, third ed. Van Nostrand Reinhold, New York.

Wong, E.W., Sheehan, P.E., Lieber, C.M., 1997. Nanobeam mechanics: elasticity, strength, and toughness of nanorods and nanotubes. Science 277, 1971–1975.

Yakobson, B.I., Avouris, P., 2001. Nanomechanics, carbon nanotubes: synthesis, structure, properties, and applications. In: Dresselhaus, M.S., Dresselhaus, G., Avouris, P. Springer-Verlag, New York, pp. 287–329.

Yakobson, B.I., Brabec, C.J., Bernholc, J., 1996. Nanomechanics of carbon tubes: instabilities beyond linear range. Physical Review Letters 76, 2511–2514.

Yakobson, B.I., Campbell, M.P., Brabec, C.J., Bernholc, J., 1997. High strain rate fracture and C-chain unraveling in carbon nanotubes. Computational Materials Science 8, 341–348.